Profiling proteomic responses to hexokinase-II depletion in terpene-producing Saccharomyces cerevisiae

Author

Lu, Z, Shen, Q, Liu, L, Talbo, G, Speight, R, Trau, M, Dumsday, G, Howard, CB, Vickers, CE, Peng, B

Published

2023

Journal Title

Engineering Microbiology

Version

Version of Record (VoR)

DOI

10.1016/j.engmic.2023.100079

Engineering Microbiology 3 (2023) 100079

Contents lists available at ScienceDirect

Engineering Microbiology

journal homepage: www.elsevier.com/locate/engmic

Original Research Article

Profiling proteomic responses to hexokinase-II depletion in terpene-producing *Saccharomyces cerevisiae*

Zeyu Lu[a,b,c,d,#], Qianyi Shen[a,b,c,e,#], Lian Liu[b,f], Gert Talbo[b,f], Robert Speight[a,c], Matt Trau[b,e], Geoff Dumsday[g], Christopher B. Howard[b], Claudia E. Vickers[a,c,d,h], Bingyin Peng[a,b,c,d,*]

[a] *ARC Centre of Excellence in Synthetic Biology, Queensland University of Technology, Brisbane, QLD, 4000, Australia*
[b] *Australian Institute for Bioengineering and Nanotechnology (AIBN), The University of Queensland, Brisbane, QLD, 4072, Australia*
[c] *Centre of Agriculture and the Bioeconomy, School of Biology and Environmental Science, Faculty of Science, Queensland University of Technology, Brisbane, QLD, 4000, Australia*
[d] *CSIRO Synthetic Biology Future Science Platform, Commonwealth Scientific and Industrial Research Organisation (CSIRO), Black Mountain, ACT, 2601, Australia*
[e] *School of Chemistry and Molecular Biosciences (SCMB), the University of Queensland, Brisbane, QLD, 4072, Australia*
[f] *Metabolomics Australia (Queensland Node), Australian Institute for Bioengineering and Nanotechnology (AIBN), The University of Queensland, Brisbane, QLD, 4072, Australia*
[g] *CSIRO Manufacturing, Clayton, VIC, 3169, Australia*
[h] *Eden Brew Pty Ltd, Glenorie, NSW, 2157, Australia*

ARTICLE INFO

Keywords:
Proteomics
Glucose repression
Metabolic engineering
Crabtree effect
Sesquiterpene
Synthetic biology
Genetic regulation

ABSTRACT

Hexokinase II (Hxk2) is a master protein in glucose-mediated transcriptional repression signaling pathway. Degrading Hxk2 through an auxin-inducible protein degradation previously doubled sesquiterpene (nerolidol) production at gram-per-liter levels in *Saccharomyces cerevisiae*. Global transcriptomics/proteomics profiles in Hxk2-deficient background are important to understanding genetic and molecular mechanisms for improved nerolidol production and guiding further strain optimization. Here, proteomic responses to Hxk2 depletion are investigated in the yeast strains harboring a *GAL* promoters-controlled nerolidol synthetic pathway, at the exponential and ethanol growth phases and in *GAL80*-wildtype and *gal80*Δ backgrounds. Carbon metabolic pathways and amino acid metabolic pathways show diversified responses to Hxk2 depletion and growth on ethanol, including upregulation of alternative carbon catabolism and respiration as well as downregulation of amino acid synthesis. De-repression of *GAL* genes may contribute to improved nerolidol production in Hxk2-depleted strains. Seventeen transcription factors associated with upregulated genes are enriched. Validating Ash1-mediated repression on the *RIM4* promoter shows the variation on the regulatory effects of different Ash1-binding sites and the synergistic effect of Ash1 and Hxk2-mediated repression. Further validation of individual promoters shows that *HXT1* promoter activities are glucose-dependent in *hxk2*Δ background, but much weaker than those in *HXK2*-wildtype background. In summary, inactivating *HXK2* may relieve glucose repression on respiration and *GAL* promoters for improved bioproduction under aerobic conditions in *S. cerevisiae*. The proteomics profiles provide a better genetics overview for a better metabolic engineering design in *Hxk2-deficient* backgrounds.

1. Introduction

Engineering microbes promises a future for the economical and sustainable production of biofuels, biochemicals, and many other biobased products [1–4]. The budding yeast *Saccharomyces cerevisiae* has been used as a common chassis organism with the advantages of well-characterized genetics and easiness of genetic modification. Through metabolic engineering and synthetic biology, yeast cells have been intensively engineered for the production of many heterologous chemicals, superior to traditional production routes such as extraction of plant and animal materials and synthesis from petroleum-derivative precursors [5–8]. Further efforts toward maximal production are undoubtedly interesting but challenging. Previous genetic modifications may dramatically interfere with global gene expression. Profiling such genetic responses may leverage better metabolic engineering designs in next-round metabolic engineering [9].

Natural *S. cerevisiae* metabolizes excess glucose into ethanol in aerobic conditions through a respiro-fermentative metabolism, and ethanol can then be re-utilized through respiration [10,11]. This metabolic pattern is known as diauxic growth, and aerobic ethanolic

* Corresponding author.
E-mail address: bingyin.peng@qut.edu.au (B. Peng).
# These authors contributed equally to this work.

https://doi.org/10.1016/j.engmic.2023.100079
Received 22 November 2022; Received in revised form 3 January 2023; Accepted 13 February 2023
Available online 3 April 2023

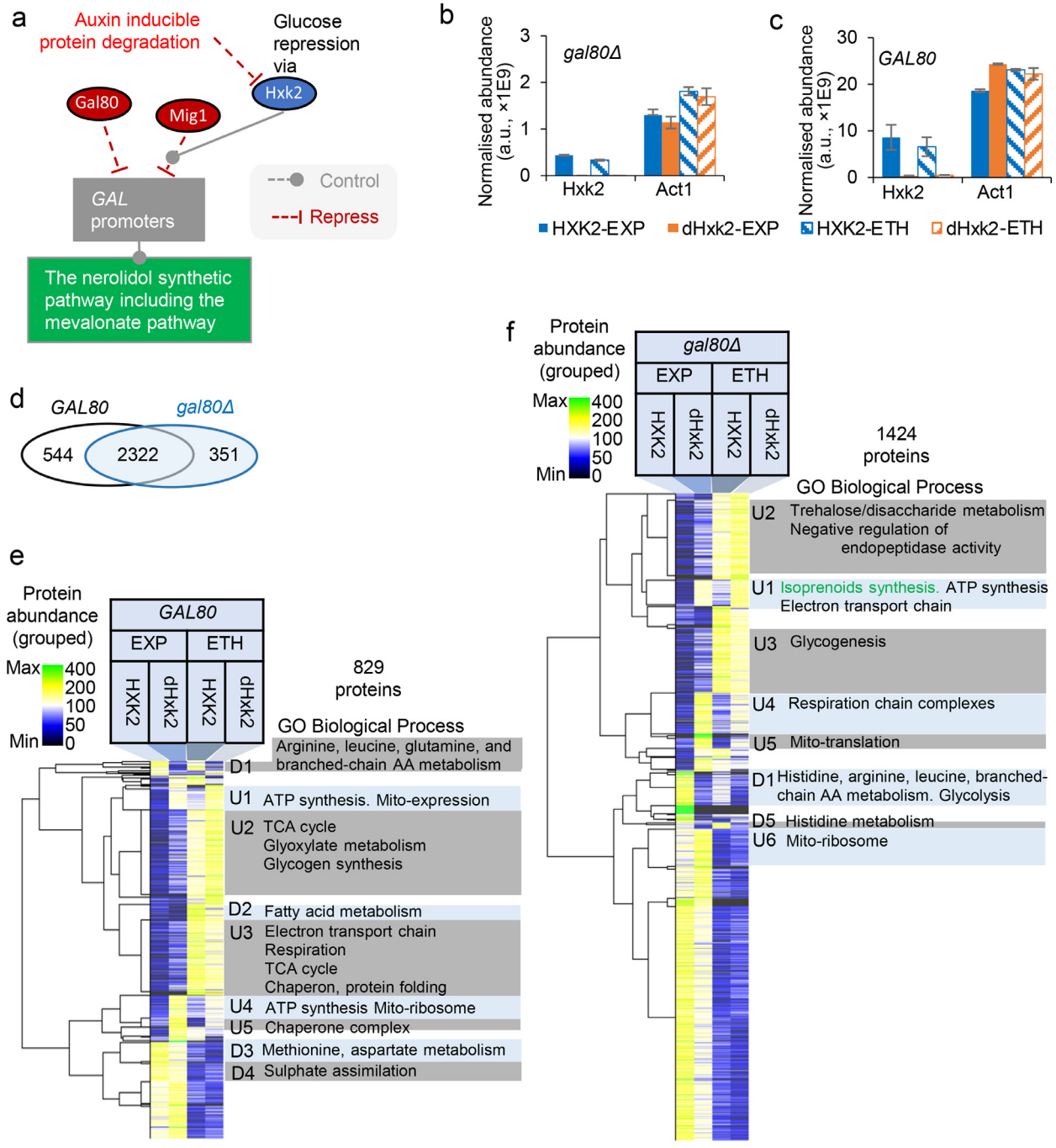

Fig. 1. Overview of proteomic responses to auxin-induced hexokinase II depletion (dHxk2) in the yeast engineered with the nerolidol synthetic pathway. (a) Genetic regulation on the nerolidol synthetic pathway. Gal80p, galactose-inducible gene repressor; Mig1p, glucose-dependent gene repressor. (b & c) Normalized abundance of Hxk2 and reference actin protein (Act1) in *gal80*Δ background and *GAL80*-wildtype backgrounds. (d) Total numbers of discovered proteins during proteomic analysis. (e & f) Clustering analysis and Gene Ontology (GO) enrichment analysis of the proteins with significant abundance change (|fold-change| ≥ 2 and *p* value ≤0.05 in any comparison : HXK2-ETH/HXK2-EXP, dHxk2-EXP/HXK2-EXP, dHxk2-EXP/dHxk2-ETH, and dHxk2-ETH/HXK2-ETH). Biological processes with enrichment factor > 10 are summarized. Yeast cells were grown in yeast nitrogen base medium with 20 g L^{-1} glucose and 100 mM 2-(N-morpholino)ethanesulfonic acid-ammonia buffer (pH = 6.0). EXP, exponential growth phase (OD_{600} ~ 2); ETH, ethanol growth phase (when OD_{600} ~10); HXK2, HXK2 wildtype; dHxk2, Hxk2 depleted through the auxin-inducible protein degradation mechanism (a); Mito, mitochondrial. Data in **c** have been published previously [21]. *N* = 3 replicates in the *GAL80* batch and *N* = 4 replicates in the *gal80*Δ batch.

fermentation is known as overflow metabolism or the Crabtree effect. Diauxic growth and overflow metabolism are regulated through glucose repression mechanisms. Through these mechanisms, alternative catabolic genes are repressed in the presence of excess glucose and induced upon glucose depletion [11,12]. In metabolically engineered terpene-producing *S. cerevisiae* strains, the galactose-inducible (*GAL*) promoters, being auto-inducible upon glucose depletion in the *GAL* repressor gene *gal80*Δ background, are used to control terpene synthetic genes (Fig. 1a) [13–15]. This contributes to improved cell growth in the exponential growth phase and to improved overall production, due to the induced higher expression output in the post-exponential growth phase, in comparison to using "constitutive" promoters [16,17]. Aiming to alleviate glucose repression on *GAL* promoter activities and respiration [18–20], we introduced an auxin-inducible protein

degradation mechanism to deplete hexokinase II (Hxk2) specifically upon auxin addition [21]. Hxk2 depletion improved trans-nerolidol (a sesquiterpene) production by ~2-fold to 3.4 g L^{-1} in flask cultivation. Previously, the global genetic responses to Hxk2 deletion were investigated through a cDNA-Affymetrix Array global transcriptomics assay [22,23] and an 84-protein proteomic analysis in wild-type CEN.PK background strain [20]. Profiling global proteomics responses would be important for a better understanding of the effects of Hxk2 disruption.

In metabolic engineering, hijacking and rewiring glucose regulatory mechanisms are common engineering strategies for improved production of non-ethanolic products, including terpenoids, fatty acids, and many other small molecules [24–26]. Apart from glucose-triggered autoinduction of *GAL* promoters in *gal80*Δ background and Hxk2 depletion/deletion, other strategies have been successful in many cases. For example, deletion of *REG1*, by encoding an Hxk2/Snf1 glucose repression pathway regulator, can increase biomass production and glycolic acid production [27]. Deletion of the downstream transcriptional repressor gene *MIG1* can also relieve glucose repression on *GAL* promoter-controlled pathways [28,29]. In non-ethanol-producing (Crabtree negative) pyruvate decarboxylase-deficient *S. cerevisiae*, the internal mutation in the negative regulator Mth1 in Snf3/Rtg2 glucose signaling pathway is important to rendering the growth phenotype and for improved production of non-ethanolic products [30]. The *Mth1/Rtg1*-regulated *HXT1* promoter showed decreased activities upon glucose depletion [31]. It has been used to control essential and flux-competing enzymes to redirect metabolic flux from growth metabolism to target metabolite synthesis [32–34]. Glucose regulatory pathways in *S. cerevisiae* are interwoven [35,36]. Hxk2 was shown to be involved in the regulation of several Mth1/Rgt1-regulated genes [37,12]. This crosstalk may cause the *HXT1* promoter to be less effective in restraining flux-competing enzyme expression in metabolic engineering.

In this study, we performed global proteomic analysis in *HXK2*-wildtype and *Hxk2*-depleted strains that are engineered with nerolidol synthetic pathways. It includes two batches of analysis: (1) in *GAL80*-wildtype background with repressed nerolidol synthesis, and (2) in *gal80*Δ background with highly active nerolidol synthesis. The impacts of Hxk2 depletion on metabolic gene expression were elaborated in the exponential growth phase and the ethanol growth phase. Transcription factor enrichment analysis was used to propose the transcription factors that might be subjected to Hxk2-dependent or Hxk2-independent regulations. Specific promoters were further characterized to validate the proteomic analysis.

2. Materials and methods

2.1. Plasmid and strain construction

Yeast strains and plasmids are listed in Supplementary Table 1. Primers are listed in Supplementary Table 2. Plasmid cloning and strain construction are described in Supplementary Table 3.

2.2. HPLC-MS/MS-based proteomics assay

Yeast cells were grown in a YNB-MES-glucose medium (6.9 g L^{-1} yeast nitrogen base without amino acids, FORMEDIUM#CYN0402; and 20 g L^{-1} glucose), in which 100 mM 2-(N-morpholino)ethanesulfonic acid (MES) was added and pH was adjusted to 6 using ammonium hydroxide. MES buffer is used to maintain the pH above 5 across the whole flask cultivation [17]. For collecting cells for LC-MS/MS-based proteomics analysis, yeast cells were first grown overnight to the exponential phase (OD_{600} between 1 and 4) in 125 mL Erlenmeyer flasks containing 15 mL YNB-MES-glucose medium. For the strains subjected to Hxk2 depletion, a synthetic auxin analog, 1-Naphthaleneacetic acid (NAA) dissolved in 100% ethanol, was added to a final concentration of 1 mM in the medium. Overnight cell cultures were then inoculated into 30 mL fresh YNB-MES-glucose medium to an initial OD_{600} of 0.2 in 250 mL flasks and grown for 48 h at 30 °C in a 200 rpm shaking incubator. For the cells with Hxk2 depletion, NAA was added again at 0 h to a final concentration of 1 mM. Cells were collected when OD_{600} was at around 2 (exponential growth phase) and above 10 (ethanol growth phase at 48 h). Collected cell samples were washed three times with phosphate-buffered saline and stored at −80 °C.

LC/MS/MS label-free proteomics were performed at Metabolomics Australia (Queensland node) and Bioplatform Australia. To prepare digested peptides for LC/MS/MS identification and quantification, a S-Trap™ Mini Spin Column Digestion Protocol was used. A total of 20 μL of eluted peptides was loaded and analyzed using an LC/MS/MS system. The peptides were analyzed by liquid chromatography-mass spectrometry. The HPLC system was an Ultimate 3000 RSLCnano (ThermoFisher, Germany). An aliquot of 2 μL sample was injected onto a trap column used for online desalting and washed at 20 μl/min prior to a resolving C18 nanoEaseTM *M/Z* CSH c18 1.7 μm (300 μm x 100 mm) column (Waters) using a 60 min gradient of 8%–95% acetonitrile in 0.1% formic acid at 300 μL/min flow rate. The eluted peptides were electro-sprayed into a Thermo Orbitrap Q Exactive HF Hybrid Quadrupole-Orbitrap Mass Spectrometer (ThermoFisher, USA). The MS parameters were for MS1 a resolution of 60,000 with scan range at 100–800 *m/z*. For MS2, the isolation window was 2.0 *m/z*, the TopN at 40, resolution at 75,000, the nAGC target at 1e6 and the max IT 40 ms. The post analysis was performed against the yeast database using the ThermoFisher Proteome Discoverer software (version 2.4).

2.3. Proteomics data analysis

Proteomics data, including normalized protein abundances (the sums of all protein abundances in each replicate are normalized to an equal) and grouped protein abundances (the sums of the normalized abundances of each protein under four comparison conditions equal to 400), were exported by ThermoFisher Proteome Discoverer software; and were processed using Microsoft Excel. The normalized protein abundances were log-transformed with two as the base ("NULL" values were replaced with "1″ for log transformation). Log-transformed values were used to calculate fold-changes and two-tailed *Welch*'s unequal variances *t*-test *p*-value. Data filtering was performed in Excel. Clustering analysis was performed using Gene-E (version 3.0.215; Broad Institute of MIT and Harvard) using the Kendall's tau distance method. Enriched biological processes were identified through Gene Ontology (GO) enrichment analysis through the Gene Ontology website (http://geneontology.org/) using the *Saccharomyces cerevisiae* database (a 2021 release) and a PANTHER™ 16.0 engine [38,39]. Regulatory matrixes and transcription factor binding sites were retrieved from the Yeastract database [40]. The *Saccharomyces* Genome Database was used to analyze the H3H4 ribosome sequences [41]. Proteomics data are deposited in Zenodo (DOI:10.5281/zenodo.7684067).

2.4. Flow cytometry

A green fluorescent protein (GFP) gene yEGFP was used as a reporter gene to examine the strength of promoters. The GFP fluorescence was analyzed using a flow cytometer (BD Accuri™ C6, BD Biosciences, USA) [17]. Yeast cells were either cultivated in 20 ml tubes or 96-well plates. YNB-MES-glucose medium was used in the cultivation.

For cultivation in 20 ml tubes, yeast cells were inoculated to an OD_{600} of 0.002 in 5 ml MES-buffered SMG media and grown overnight to the exponential phase (OD_{600} around 1) for measuring the GFP fluorescence . For cultivation in 96-well plates, yeast cells were inoculated into 100 μl SMG media and grown overnight to prepare the seed cultures. The seed cultures were diluted 20 times into 100 μl MES-buffered SMG media (OD_{600} around 0.4) and grown for 24 h for measuring the GFP fluorescence at the ethanol growth phase. The seed cultures were diluted 1000 times into 100 μl MES-buffered SMG media (OD_{600} around

0.008) and grown overnight (around 18 h) for measuring the GFP fluorescence at the exponential growth phase (OD_{600} around 1 to 2).

The cultures at the exponential phase were directly analyzed. The cultures at the ethanol growth phase were diluted ten times using water before analysis. FSC.H threshold (250,000) was applied to exclude debris particles. The GFP fluorescence was excited by a 488 nm laser and detected with a 530/20 bandpass filter at the FL1.A channel. The forward scatter (FSC.A) and the side scatter (SSC.A) were also extracted and used to normalize the GFP fluorescence between different samples. The GFP fluorescence was expressed as the fold of the autofluorescence in the exponential growth phase cells of strain GH4 [17] or CEN.PK113–7D [42].

3. Results and discussion

3.1. Overview of proteomics analysis

We previously introduced a heterologous sesquiterpene (*trans*-nerolidol) synthetic pathway in *S. cerevisiae* CEN.PK2–1C [7,16,21]. This pathway comprises eleven enzymes (acetyl-CoA synthase *Acs2*, hydroxy-methylglutaryl-CoA synthase *mvaS*, hydroxy-methylglutaryl-CoA reductases *mvaE* & $HMG2^{K6R}$, 2 × mevalonate kinase *Erg12*, phosphomevalonate kinase *Erg8*, mevalonate pyrophosphate decarboxylase *Mvd1*, isopentenyl diphosphate:dimethylallyl diphosphate isomerase *IDI1*, farnesyl pyrophosphate synthase *ERG20*, and nerolidol synthase *NES1*), which are expressed under the control of *GAL* promoters; and three enzymes (*Erg8, Mvd1*, and *Idi1*) under the control of "constitutive" promoters (Figs. 1a and 2). Combining with the deletion of the GAL repressor gene *GAL80*, the yeast strain produced ~1.7 g L^{-1} nerolidol. Hexokinase II (Hxk2) deletion may relieve glucose repression on *GAL* promoters and respiration metabolism and increase biomass production [18–20]. We hypothesized that disrupting hexokinase II (Hxk2) may improve nerolidol production in this strain. We then introduced an auxin inducible protein degradation mechanism to deplete, which resulted in the production of ~3.4 g L^{-1} nerolidol, a two-fold improvement [21]. We previously employed HPLC-MS/MS-based label-free proteomics to confirm the depletion of Hxk2 upon auxin addition (Fig. 1b) [21]. However, the whole proteomics data were not analyzed and published. In this study we further analyzed the samples of this batch of proteomics under four conditions: (1) exponential growth phase in *HXK2* wild-type background (HXK2-EXP), (2) exponential growth phase in Hxk2-depleted background (dHxk2-EXP), (3) ethanol growth phase in *HXK2* wild-type background (HXK2-ETH), and (4) ethanol growth phase in Hxk2-depleted background (dHxk2-ETH). In total, 2673 proteins were identified with quantitative data (Fig. 1d: *gal80*Δ). Aiming to get a better understanding of Hxk2 depletion-mediated genetic and metabolic responses, we performed an in-depth data analysis.

To profile the genetic response in the absence of the metabolic interference of the heterologous nerolidol synthetic pathway, we further analyzed the proteomics under the same four conditions in the *GAL80*-wildtype isogenic strains (Fig. 1c). In this batch of proteomics, 2866 proteins were identified with quantitative data. The *GAL80* batch of data and the *gal80*Δ batch of data were collected by using two different sets of HPLC-MS/MS equipment, which vary in the electrospray interface and HPLC-column running time. We found that it is not reliable to co-analyze them as one batch. We therefore analyzed two batches of data separately. Both batches of data share 2322 identified proteins (Fig. 1d; Supplementary dataset 1). To validate the proteomics data consistency in replicate experiments, we performed clustering analysis on the normalized protein abundance data for all samples (Supplementary Fig. 1). These samples were split into four clusters, in which the replicates were clustered together consistently with the four test conditions. To evaluate the significance of the change, we used *Welch*'s unequal variances *t*-test, which is known as having the type-I error (false positive) robustness [43], to calculate the *p* value independently.

We first selected the proteins that showed |fold-change| ≥ 2 and *p* value ≤0.05 (two-tailed *Welch*'s test of log-transformed data) in any of the following four sets of comparison: (1) HXK2-ETH/HXK2-EXP, (2) dHxk2-EXP/HXK2-EXP, (3) dHxk2-EXP/dHxk2-ETH, and (4) dHxk2-ETH/HXK2-ETH. There were 829 proteins selected in the *GAL80* dataset and 1424 proteins in the *gal80D* dataset (Fig. 1e and f). The grouped abundance data of the filtered proteins were clustered and analyzed through GO biological process enrichment (Fig. 1e and f).

Partial de-repression and nearly full de-repression of the expression of some proteins were shown in EXP-dHxk2 conditions. For partial de-repression, proteins from the tricarboxylic acid (TCA) cycle and the pathways for glycogen synthesis, glyoxylate metabolism, and respiratory metabolism were enriched in *GAL80* background (Fig. 1d: cluster U2 & U3), and proteins from the pathways for glycogenesis and trehalose/disaccharide metabolism were enriched in *gal80*Δ background (Fig. 1f: clusters U2 & U3). For full de-repression, proteins involved in mitochondrial respiration, ATP synthesis, and protein expression were enriched in *GAL80* and *gal80*Δ background (Fig. 1e and f: clusters U1, U4, & U6). In the *gal80*Δ background, the proteins enriched for isoprenoid synthesis are the proteins from the engineered nerolidol synthetic pathway. This confirmed that the depletion of hexokinase II lifts glucose repression on *GAL* promoters-controlled heterologous synthetic pathway. It also indicated that upregulated expression of mitochondrial respiration machineries relates to the de-repression of respiration in *hxk2*Δ background, i.e., improved growth during the ethanol growth phase [21].

In EXP-dHxk2 conditions, proteins involved in amino acid synthesis showed decreased abundance (Fig. 1e and f: cluster D1, D3, D4, & D5). There were more down-regulated proteins in the *gal80*Δ background than in the *GAL80* background, including cluster D1 in the *gal80*Δ background (Fig. 1f) vs. cluster D1 in the *GAL80* background (Fig. 1e). Down-regulated glycolytic proteins were enriched in the *gal80*Δ background (Fig. 1f: cluster D1) but not in the *GAL80* background.

3.2. Responses of carbon metabolic pathways to HXK2 depletion and growth on ethanol

Deletion of HXK2 can cause a series of metabolic effects, including decreasing fermentation capacity on glucose [23], increasing fermentation capacity on maltose [23], enabling simultaneous utilization of glucose and galactose, increasing respiratory tricarboxylic acid (TCA) cycle activities [20], and 2-fold improvement of nerolidol production in metabolically engineered yeasts [21]. Here, we illustrate the relative abundance of the proteins from the relevant carbon metabolic pathways (Fig. 2).

The proteomics responses to Hxk2 depletion on glucose (EXP) showed many consistencies with the previous transcriptomics studies [22,23], including upregulated expression of the tricarboxylic acid cycle and electron transport train components (Fig. 2). There were some differences, such as Fbp1, and Pck1. This may be due to different cultivation conditions, different background strains, and other experimental conditions. Consistent with a previous study [44], Hxk2 depletion upregulated other hexokinases (Glk1, Hxk1, and Emi2). Catabolic proteins for the utilization of alternative carbon sources, including sucrose, maltose (in *gal80*Δ background), sorbitol, and galactose (in *gal80*Δ background) showed upregulation. Double deletion of *HXK2* and *HXK1* enabled invertase Suc2 expression [45]. Consistent with another previous study [46], depletion of Hxk2 alone may derepresses Suc2 expression (Fig. 2), Hxk2 depletion only slightly increased the proteins from trehalose and glycogen metabolism in the presence of glucose, and glucose depletion was important for their de-repression.

The abundance changes of hexose transporters had different patterns, including glucose-dependent expression of Hxt1 and Hxt3, and

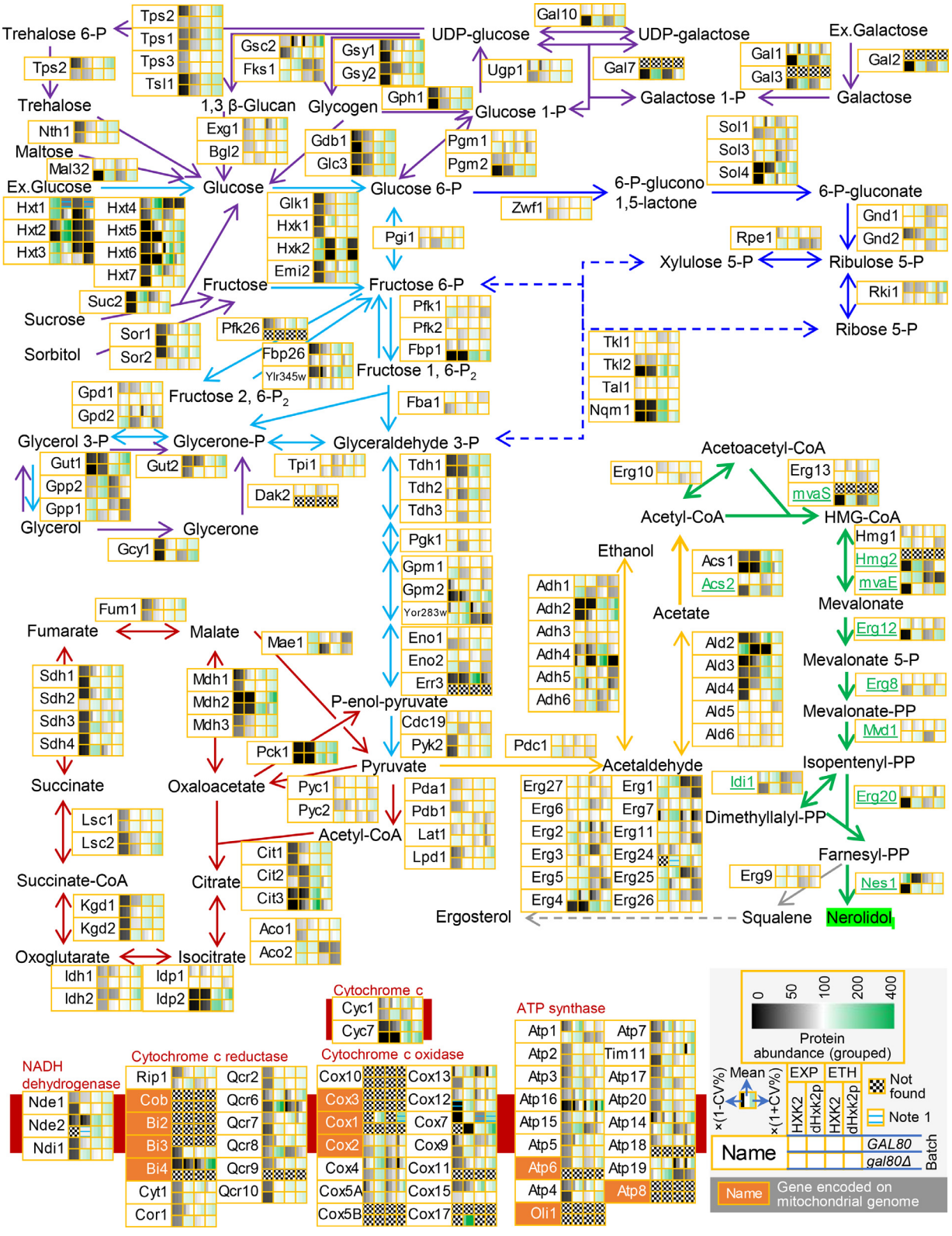

Fig. 2. Relative protein abundances in the carbon hydrate metabolic pathways, the tricarboxylic acid cycle, respiratory electron transfer train, and the terpenoid synthetic pathway. *GAL* promoters are used to control the expression of underlined proteins. Arrow colors: purple, alternative carbon hydrate utilization; cyan, glycolysis; yellow, ethanol/acetyl-CoA related metabolism; green, engineered nerolidol synthetic pathway; red, the citric acid cycle. Mean, the mean value of grouped protein abundance; CV, the coefficient of variation; $N = 3$ replicates in the *GAL80* batch and 4 replicates in the *gal80*Δ batch. Ex., extracellular. Note 1: proteins in two or three biological replicates are not found, and the coefficient of variation (CV) is not available.

glucose repression on Hxt5, Hxt6, and Hxt7. Hxk2 depletion led to ~4-fold decrease in Hxt1 protein abundance (Fig. 2: in *gal80*Δ background; not detected in two biological replicates in *GAL80* background) and >7-fold increase in the abundance of Hxt2 and Hxt4 in the exponential growth phase (Fig. 2). These were consistent with the changes in their promoter activities in *the hxk2*Δ background [47]. This consistency may validate the reliability of proteomics data in the current study.

In the nerolidol synthetic pathway, proteins are expressed under the control of *GAL* promoters (Fig. 2: Acs2, MvaS, mvaE, $Hmg2^{K6R}$, Erg12, Erg8, Mvd1, Idi1, Erg20, and Nes1). Hxk2 depletion induced their expression levels in the *gal80*Δ background. Previously, a fluorescent protein reporter (*Y-FAST*) was expressed together with Nes1 under the control of the *GAL2* promoter [21]. Y-FAST fluorescence at the single-cell levels was typically consistent with its protein abundance. The *GAL* promoter-controlled nerolidol synthetic pathway enzymes as well as the enzymes from the endogenous galactose utilization pathway (Fig. 2: Gal2, Gal1, Gal3, Gal10, and Gal7) had increased abundance in response to Hxk2 depletion during the exponential growth phase and the ethanol growth phase, consistent with the improved production during both phases [21]. These data validate our previous hypothesis that Hxk2 depletion may upregulate the *GAL* promoter-controlled pathway and may explain the improved nerolidol production caused by Hxk2 depletion.

In Hxk2-depletion conditions, Hxt1p abundance was maintained at similar levels in the exponential growth and ethanol growth phases. Hxt1 abundance on ethanol growth was ~15-fold higher in the Hxk2 depletion background than in the *HXK2*-wildtype background. This suggests that the *HXT1* promoter is not suitable for dynamic gene expression control in metabolic engineering in Hxk2-depleted/*hxk2*Δ background. In the Hxk2 depletion background, Hxt3 abundance showed a ~40-fold decrease in ethanol in the *GAL80*-wildtype background and a ~5-fold decrease in the *gal80*Δ background. This indicates that the Hxt3 promoter can also be used as a dynamic control in an Hxk2-depleted background, as shown previously [48].

Proteins in the tricarboxylic acid (TCA) cycle are either induced by Hxk2 depletion or induced in the ethanol growth phase. Most mitochondrial respiratory electron transfer chain proteins are induced by Hxk2 depletion, including the Cox2 that is encoded in the mitochondrial genome. The components for mitochondrial translation machineries showed increased protein abundance in response to Hxk2 depletion or growth on ethanol (Supplementary Fig. 2). This shows that Hxk2 depletion upregulates mitochondrial functions. Mitochondria are important subcellular organelles for engineering heterologous biosynthetic pathways [49]. Upregulated TCA cycles, respiration, and mitochondrial expression can be harnessed for mitochondrial metabolic pathway optimization.

For the major isoenzymes in the glycolytic pathway (Pgi1, Pfk1, Pfk2, Fba1, Tpi1, Tdh3, Pgk1, Gpm1, Cdc19, and Pdc1; except of Eno2), protein abundances were stable in the four test conditions in the *GAL80*-wildtype background (Fig. 2). In the *gal80*Δ background, Hxk2 depletion resulted in decreased abundance for Tdh3, Pgk1, Gpm1, Eno2, and Cdc19 in the exponential growth phase (fold-change > 2; $p < 0.05$). Previous work had shown that Hxk2 depletion caused slower growth in the *gal80*Δ nerolidol-producing strain [21]. It is not certain whether downregulation of glycolytic pathway enzymes is related to the metabolic burden caused by overexpression of the nerolidol synthetic pathway.

For downstream ergosterol synthesis, the change patterns for different enzymes varied in response to Hxk2 depletion or growth on ethanol. Erg1 abundance decreased in the ethanol growth phase. It is not clear whether it is regulated by the Erg1 protein degradation mechanism [50,51]. Erg4 catalyzes the final step for ergosterol synthesis. In the *gal80*Δ background, its protein levels in ethanol-phase cells are ~20- or-30-fold higher than those in exponential-phase cells. The regulatory mechanism of this change is also not clear.

3.3. Responses of amino acid metabolic pathways to Hxk2 depletion and growth on ethanol

GO enrichment showed decreased protein abundance in several amino acid metabolic pathways in response to Hxk2 depletion (Fig. 1d and f). Here, we summarized the data for proteins in amino acid metabolic pathways (Fig. 3).

In Hxk2-depleted cells, the enzymes from leucine, valine, isoleucine, and arginine synthetic pathways showed decreased abundance in *GAL80* and *gal80*Δ backgrounds and exponential and ethanol growth phases, in comparison to that in *HXK2*-wildtype cells (Fig. 3). Enzymes for histidine synthesis showed >2-fold decrease in several conditions, i.e., His4 and His7 in *gal80*Δ background during the exponential growth phase, His3 in *GAL80* background during the exponential growth phase, and His5 in *gal80*Δ background during the ethanol growth phase. Some enzymes for the synthesis of other amino acids (i.e., Glt1, Gln1, Ser33, Aat1, Aat2, etc.) also showed decreased abundance in response to Hxk2 depletion under several conditions. The abundance of some enzymes from the lysine synthetic pathway and the sulfate assimilating pathway slightly decreased in response to Hxk2 depletion but showed *a* >2-fold decrease in the ethanol growth phase in comparison to the exponential growth phase (Fig. 3). This shows that amino acid synthetic pathways are downregulated in response to Hxk2 depletion or growth on ethanol.

The enzymes involved in the degradation of glutamate and proline showed increased protein levels in the ethanol growth phase in comparison to the exponential growth phase (Fig. 3: Gdh2, Gad1, Uga1, Uga2, and Put2). This suggests that glucose repression is applied to these amino acid degradation pathways.

The induction patterns for Uga2 in *GAL80*-wildtype and *gal80*Δ cells were different. In *GAL80*-wildtype cells, Uga2 abundance was ~3-fold higher in the ethanol-growth phase than that in the exponential growth phase (not influenced by Hxk2 depletion). In *gal80*Δ cells, Uga2 abundance was at similar levels in the ethanol-growth phase (not influenced by Hxk2 depletion), was ~2-fold higher than that in the exponential growth phase in *HXK2* wildtype. Uga2 abundance was ~12 fold higher in the exponential phase in Hxk2-depleted cells than in *HXK2*-wildtype cells ($p = 0.001$). The divergent patterns were also seen for Lys1 and Gly1. For Gly1: in *GAL80* cells, protein abundance increased in response to Hxk2 depletion and growth on ethanol, and in *gal80*Δ cells, protein abundance decreased. The regulation mechanisms for these change patterns are not clear.

These data show that the enzymes in amino acid metabolism are regulated by Hxk2-dependent or Hxk2-independent regulatory mechanisms.

3.4. Transcriptional factor enrichment analysis

The protein expression profiles indicate that there are Hxk2-dependent and Hxk2-independent mechanisms in the regulation of carbon hydrate, energy, and amino acid metabolism. To have a better understanding of regulatory mechanisms, we further performed transcription factor enrichment analysis.

We separately retrieved the regulatory matrixes of the genes listed in two batches of proteomics analysis from the Yeastract database. The matrixes include the Boolean data of "documented binding or expression evidence" of 207 transcription factors on each gene. To analyze the association between each transcription factor and its potential genetic regulation, we calculated the difference in the ratios of upregulated genes and downregulated genes in total targets (Fig. 4a and b: Δratio). We set the "upregulated" and "downregulated" thresholds as $|\log_2\text{fold-change}| \geq 1$ and two tailed Welch's test *p*value ≤0.1. We calculated the Δratio in the four comparison conditions: (1) in *HXK2*-wildtype background, ETH (the ethanol growth phase) vs. EXP (the exponential growth phase), (2) under EXP conditions, dHxk2 (Hxk2-depleted background) vs. *HXK2* (*HXK2*-wildtype background), (3) in dHxk2 background, ETH vs. EXP, and (4) under ETH conditions, dHxk2 vs. *HXK2*. These four comparison

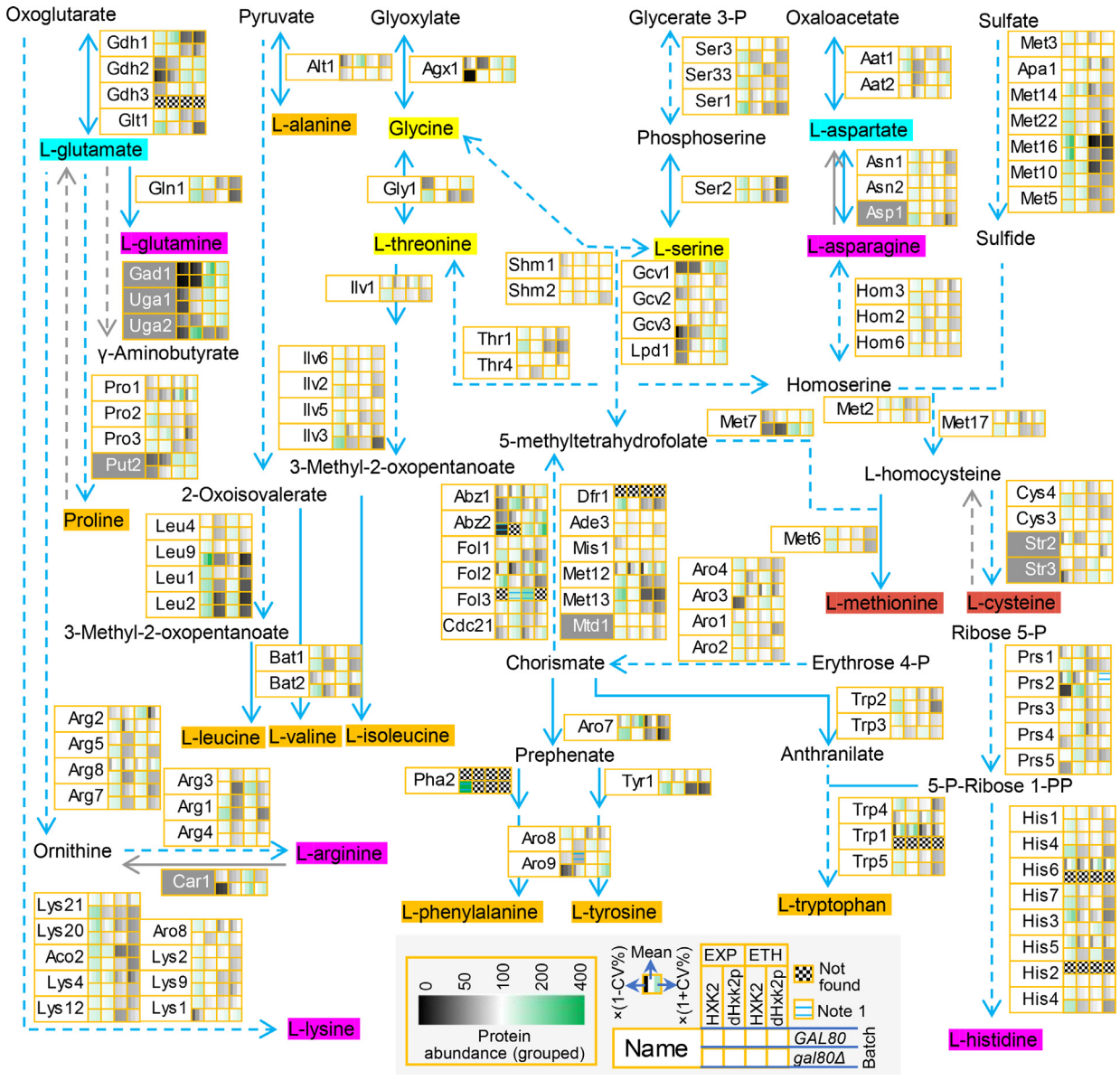

Fig. 3. Relative protein abundances in the amino acid metabolic pathways. Mean, the mean value of grouped protein abundance; CV, the coefficient of variation; $N = 3$ replicates in the *GAL80* batch and 4 replicates in the *gal80*Δ batch. Note 1: proteins in two or three biological replicates are not found, and CV is not available.

conditions may allow the cross-examination of the transcription factor responses to Hxk2 depletion and growth on ethanol. The transcription factors with a $|\Delta ratio| \geq 0.3$ are shown (Fig. 4a and b). The transcription factors matching with the filtering conditions are those associated with the upregulated genes (positive Δratio).

Through the transcription factor enrichment analysis, the enriched transcription factors included Cat8p, Gis1p, Mig1p, Nrg1p, Nrg2p, Stb3p, Sut2p, and Tog1, which had been previously characterized as the factors important for glucose repression or non-fermentable carbon source utilization. Other enriched transcription factors were Ash1p, Com2p, Gat4p, Hot1p, Rds1p, Rgm1p, Stp2p, Wtm2p, and Yap6p. None of these transcription factors responded to Hxk2 depletion during the ethanol growth phase (Fig. 4a and b), which might be due to the fact that glucose repression, including Hxk2-mediated repression, is relieved on ethanol.

Com2p shares some DNA-binding sites with Nrg1p and Gis1p (Yeastract-TF-Consensus list) [52]. Its enrichment is associated with the upregulation of the proteins in trehalose metabolism (Pgm2, Tps2, and Tsl1), glycogen metabolism (Pgm2, Gsy1, Gsy2, and Igd1), mitochondrial metabolism (Gpd1, Cit1, Ndi1, Nde1, Atp5), and others such as Uga2 (Figs. 2 and 3). Ash1p is a *trans*-repressor that works through the Rpd3L histone deacetylase complex and regulates *HO* transcription and pseudohyphal growth [53,54]. Gat4p is involved in spore wall assembly and zinc ion starvation [55]. Wtm2p is involved in regulation of meiosis, response to replication stress, and hypoxia [56]. Rgm1 is also involved in response to hypoxia [57].

Hot1 is an important activator in the osmotic stress response HOG (High Osmolarity Glycerol) pathway [58]. Glucose starvation can activate the HOG pathway, which does not critically depend on Snf1 [59]. This might help to explain the stronger activation response by Hot1 to growth on ethanol in comparison to the response to Hxk2 depletion. Furthermore, Hot1 co-regulates ~88% target genes, such as *HSP12, RTC3*, and *ALD3*, together with Ras/cAMP pathway downstream transcription factors Sko1 and Msn2/Msn4 [60–63]. Hsp12, Rtc3, and Ald3 showed increased abundance in response to Hxk2 depletion in the exponential growth phase and in response to growth on ethanol. The Ras/cAMP pathway has a crosstalk with the HOG pathway via Ras2-Cdc42-Ste20 [63,64].

a

Δratio in *GAL80* background

Transcription factor [Note 1]	No. Of found targets [Note 2]	HXK2 (ETH/EXP)	EXP (dHxk2/HXK2)	dHxk2 (ETH/EXP)	ETH (dHxk2/HXK2)
Ash1	96	0.34	0.16	0.18	0.01
Cat8	85	0.48	0.21	0.36	-0.02
Com2	92	0.33	0.22	0.16	0.01
Gat4	197	0.35	0.26	0.13	0.01
Gis1	305	0.40	0.20	0.21	-0.04
Hot1	25	0.64	0.24	0.48	-0.12
Mig1	262	0.31	0.23	0.16	0.02
Nrg1	152	0.26	0.24	0.03	0.01
Nrg2	71	0.52	0.44	0.17	-0.01
Rds1	95	0.31	0.22	0.15	0.00
Rgm1	283	0.31	0.22	0.16	0.01
Stb3	17	0.41	0.47	0.06	0.12
Stp2	210	0.32	0.18	0.13	-0.01
Sut2	121	0.33	0.21	0.07	0.04
Tog1	125	0.34	0.21	0.23	-0.02
Wtm2	77	0.42	0.31	0.25	0.04
Yap6	25	0.08	0.16	-0.04	0.04

b

Δratio in *gal80Δ* background

Transcription factor [Note 1]	No. Of found targets [Note 2]	HXK2 (ETH/EXP)	EXP (dHxk2/HXK2)	dHxk2 (ETH/EXP)	ETH (dHxk2/HXK2)
Ash1	87	0.24	0.20	0.13	-0.03
Cat8	82	0.43	0.23	0.23	-0.10
Com2	89	0.13	0.24	0.07	0.02
Gat4	184	0.24	0.35	0.11	0.02
Gis1	266	0.32	0.30	0.18	-0.02
Hot1	24	0.67	0.33	0.54	0.00
Mig1	243	0.33	0.25	0.15	0.02
Nrg1	138	0.16	0.31	-0.05	0.04
Nrg2	64	0.45	0.53	0.03	0.00
Rds1	102	0.08	0.20	-0.01	0.02
Rgm1	279	0.17	0.22	0.08	-0.01
Stb3	17	0.29	0.35	0.06	0.12
Stp2	188	0.20	0.27	0.15	0.02
Sut2	112	0.23	0.27	0.05	0.00
Tog1	123	0.15	0.20	0.09	-0.02
Wtm2	76	0.24	0.33	0.13	0.01
Yap6	24	0.13	0.33	-0.04	0.17

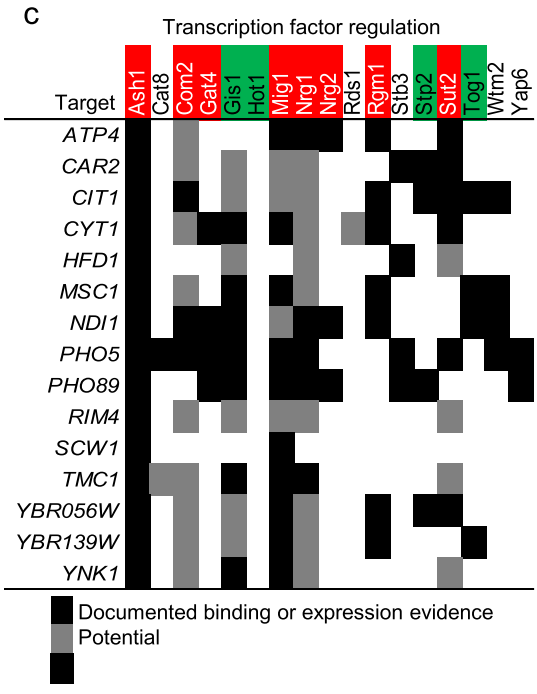

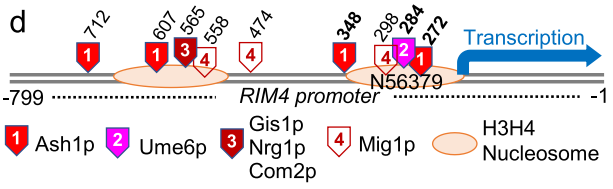

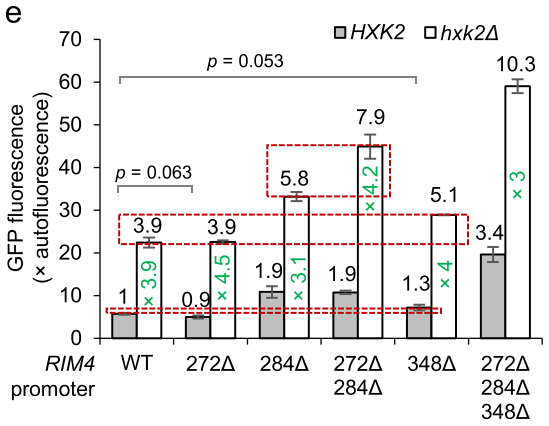

Fig. 4. Transcription factor enrichment analysis and validation of Ash1-mediated regulation on the *RIM4* promoter. (a & b) the ratio difference (Δratio) of upregulated and downregulated targets for enriched transcription factors. The factors with a $|\Delta ratio| \geq 0.3$ are shown (Note 1, except of the one with shadow). Note 2, the factors in black font and green shadow are activators, and the factors in white font and red shadow are repressors. (c) Regulation by enriched transcription factors on Ash1 targets that are upregulated in response to Hxk2 depletion in *gal80*Δ background and the exponential growth phase. The data for "documented binding or expression evidence" and "Potential" regulation are retrieved from the Yeastact database. (d) The landscape of the *RIM4* promoter structure. (e) Effects of the removal of Ash1 and Ume6 binding sites on the *RIM4* promoter activities in *HXK2* and *hxk2*Δ background and the exponential growth phase. The numbers at the top of the bars are the fold-changes relative to the wildtype (WT) *RIM4* promoter in *HXK2*-wildtype cells. The numbers in the unfilled bars are the fold-changes of the activities in *hxk2*Δ cells relative to *HXK2*-wildtype cells.

Stp2p is the transcription activator in response to extracellular amino acid through Ssy1p-Ptr3p-Ssy5p (SPS) sensor, which activates the amino acid permease expression [65]. The high-affinity glutamine permease gene *GNP1* is a Stp2p regulation target. In the *gal80*Δ background, it can only be detected in Hxk2-depleted cells during the exponential growth phase. In the same comparison conditions, the fold-change for another target Mup1, the high-affinity methionine transporter, is not significant. Other amino acid transporters are below the detection limit. In the *GAL80* background, most of amino acid permeases have lower protein abundance in response to Hxk2 depletion and growth in ethanol. This may indicate that Stp2 enrichment is not related to the extracellular amino acid sensing pathway. Upregulated targets of Stp2 in response to growth on ethanol include amino acid utilization proteins (i.e., Gdh2, Gdh3, Bna5, Car2, Gcv1, Gad1, etc.). Carbon starvation inducing amino acid utilization is a well-known physiological phenomenon. However, it is not clear whether Stp2 crosstalks with the glucose sensing pathway to regulate the amino acid utilization pathway. Further investigation is necessary.

Many proteins have decreased abundance in response to Hxk2 depletion and growth on ethanol. To investigate the possibility of downregulation being associated with certain transcription factors, we recalculated the Δratio with decreased thresholds: $|\log_2\text{fold-change}| \geq 0.5$ and two tailed *Welch*'s test *p*value ≤0.1 (Supplementary Table 4). In the *GAL80* background, Ifh1p and Lys14p are enriched with a Δratio <−0.3. In the *gal80*Δ background, additional factors are enriched, including Asg1p, Fkh2p, Gsm1p, Ime1p, Ndt80p, Ure2p, and Yrm1p. Enrichment of Lys14p is due to the downregulation of Lys2, Lys4, Lys9, Lys12, and Lys20 (Fig. 3).

It is challenging to bring more details to the signaling pathways that link the triggers (Hxk2 depletion or growth on ethanol) and the protein expression changes. The transcription factor enrichment analysis may contribute to adding clues to the elucidation of the regulatory pathways. Further investigation is necessary to confirm the roles of enriched transcription factors and the states of their upstream signaling pathways.

3.5. *Hxk2-dependent repression and Ash1-mediated repression on the* RIM4 *promoter*

Ash1 is one of the enriched transcription factors that may be associated with expression upregulation in response to Hxk2 depletion and growth on ethanol. Ash1 stability is regulated by cyclin-dependent Pho80-Pho85 kinase complex [66] and Ash1 mRNA translation is regulated by Phd1, which is regulated by the glucose sensors Snf3/Rgt2-regulated Yck1 kinase [67] and cyclin-dependent Ssn3 (Cdk8) kinase [68]. There were the hypotheses about the interaction of Snf1 regulation with Cdk8 [68] and Pho85 [69]. To investigate the potential regulatory role of Ash1 in response to Hxk2 disruption, we analyzed the Ash1 targets that were upregulated in response to Hxk2 depletion (Fig. 4c, *gal80*Δ batch). According to the regulatory matrix, based on "documented binding or expression evidence", *RIM4* is the Ash1 target that is not regulated by other enriched factors. We therefore chose the *RIM4* promoter for further validation.

In the *RIM4* promoter region, there are two H3H4 nucleosomes [41] and the binding sites for Ash1, Mig1, Gis1, Nrg1, and Com2 (Fig. 4d). This is not consistent with the regulatory matrix data based on "documented binding or expression evidence" (Fig. 4c). We then re-retrieved the regulatory matrix based on "Potential" evidence. Consistently, the "potential" regulatory matrix indicates that *RIM4* is the target of Mig1, Gis1, Nrg1, and Com2. This indicates that considering the transcription factors based on "potential" evidence could be important for the enrichment analysis. We decided to continue to dissect the *RIM4* promoter and understand the role of Ash1 in the *RIM4* promoter activities. Our hypothesis was that if Hxk2 deficiency may relieve Ash1-mediated repression fully, the *RIM4* promoter, and its mutant with all Ash1-binding sites removed would behave similarly in Hxk2-deficient cells.

We focused on the Ash1 sites in the nucleosome N56379 region, from where the *RIM4* transcript starts (Fig. 4d). In the nucleosome N56379 region, there is a Ume6-binding site. Ash1 and Ume6 have been found being co-active in recruiting the Rpd3 histone deacetylase complex (Fig. 4d) [70,71]. Therefore, Ash1 and Ume6 sites were removed individually or combinatorially (Fig. 4e). We then cloned the *RIM4* promoter and its mutants upstream of the reporter yEGFP gene, and yEGFP was under the control of the *PGK1* terminator [28]. The yEGFP expression cassettes were integrated at the *ura3* locus into CEN.PK113–5D (*HXK2* wildtype) [42] and its *hxk2*Δ mutant, separately. The GFP fluorescence was measured to indicate the expression outputs from the *RIM4* promoter and its mutants (Fig. 4e).

In *HXK2* wildtype cells, removing any individual Ash1 site 272 or 348 did not cause a big change in the *RIM4* promoter activities, removing Ume6 site 284 doubled the *RIM4* promoter activities, and combinatorial removal of the sites 272, 284, and 348 further increased the promoter activities (Fig. 4e). This shows that *RIM4* is repressed through Ash1 and Ume6-mediated mechanisms.

In *hxk2*Δ cells, removing Ash1 site 274 did not influence the *RIM4* promoter activities, whereas removing Ash1 site 348 increased its activities by 30% (Fig. 4e). This shows that different Ash1 sites have varied epigenetic effects on repressing the *RIM4* promoter. In the absence of Ume6 site 284, removing Ash1 site 274 increased the *RIM4* promoter activities in *hxk2*Δ cells but not in *HXK2*-wildtype cells (Fig. 4e). Derepression effect caused by Ash1 site 348 removal is more significant in *hxk2*Δ cells. These indicate the synergistic regulation on the *RIM4* promoter by Ash1-mediated repression and Hxk2-dependent repression mechanism, which can function through Mig1 site 298.

The data in the current work are not sufficient to show whether Hxk2 depletion may alleviate Ash1-mediated repression. A systematic investigation is necessary to validate this hypothesis. However, we confirmed that the *RIM4* promoter is co-repressed by the Hxk2-dependent mechanism and the Ash1-Ume6-mediated mechanism.

3.6. *Regulatory promoters that respond to Hxk2 depletion or growth in ethanol*

In metabolic engineering, regulatory promoters are used to dynamically control the expression of heterologous genes [72,17]. Gene expression is regulated at multiple levels. This regulation may influence the correlation between target protein abundance and the activity of the promoter that controls the target protein gene transcription. Validating the activities of the potentially applicable promoters is important for future genetic design. Here, we further characterized the activities of eleven promoters in *HXK2*-wild background strains and *hxk2*Δ background strains (Fig. 5a).

We constructed a new vector system for promoter characterization. In this system, the yEGFP expression cassettes controlled by the target promoter and the *PGK1* terminator were integrated into the genome and substituted with the whole *HML* locus. The *HML* locus was naturally silenced through sirtuins-dependent mechanisms [73,74]. The promoter test would not be influenced by *HML*-related genome-silencing mechanisms, since the whole *HML* locus was replaced. Three strong constitutive promoters for *TDH3, ADH1*, and *TEF1* genes were re-characterized to validate the system. Their strength patterns were consistent with our previous observations [17].

Other promoters were selected according to the protein abundance responses in the proteomics data (Fig. 5b and Supplementary Fig. 3). For example, Tdh1 and Mdh1 abundances increased in response to growth on ethanol, with no, or moderate responses to Hxk2 depletion. Hxt7 abundance increased in response to either Hxk2 depletion or growth on ethanol. Met16, Bud20, and San1 abundances decreased in response to growth on ethanol and did not respond to Hxk2 depletion. Hxt1 abundance decreased in response to either Hxk2 depletion or growth on ethanol.

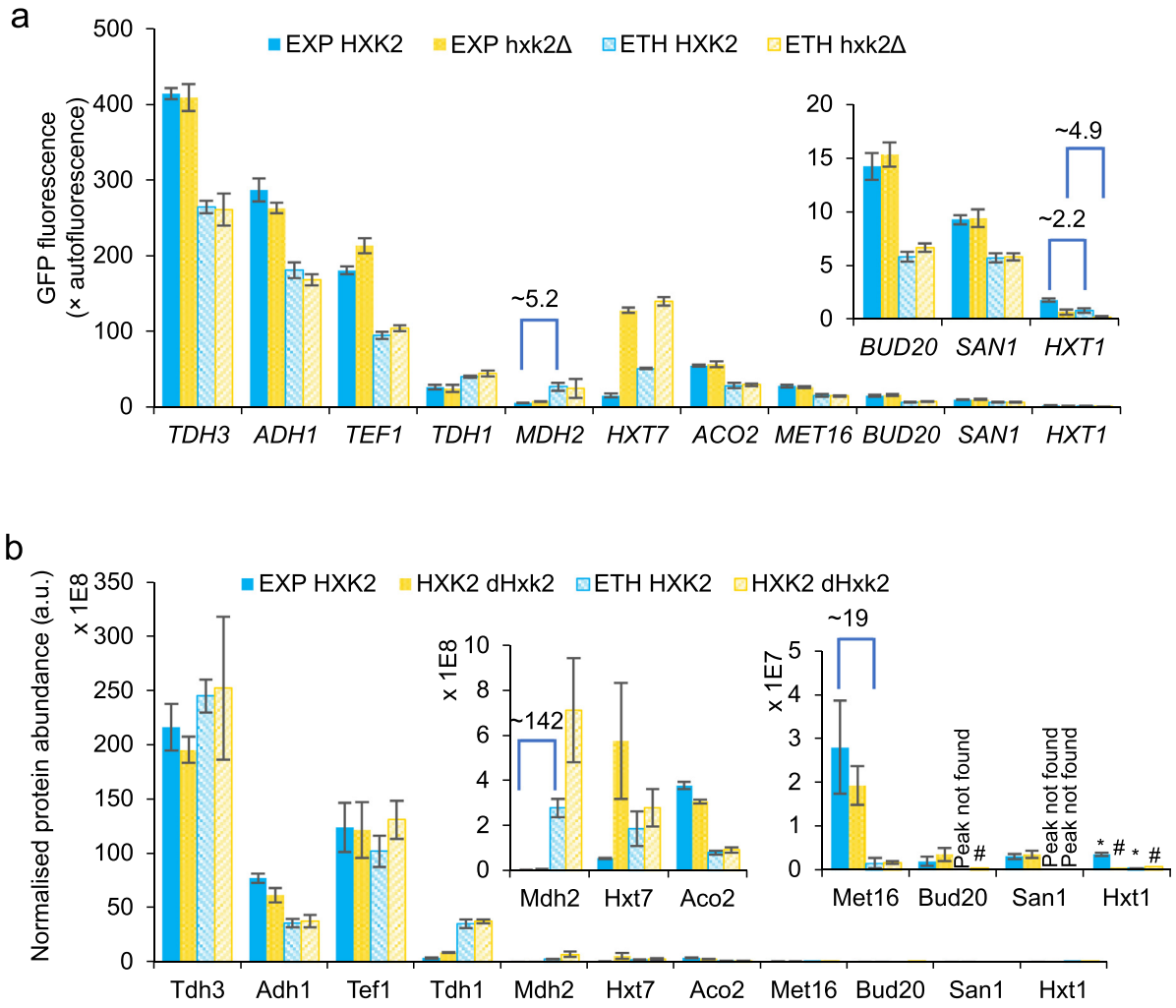

Fig. 5. Validating the effects of disrupting Hxk2 on the expression of eleven promoters. (a) Promoter characterization in *HXK2*-wildtype background and *hxk2*Δ background. (b) Normalized protein abundances in *HXK2*-wildtype background and Hxk2-depleted (dHxk2) background from proteomics data in the *GAL80* batch. The numbers above the bars are the absolute fold-changes. EXP, exponential growth phase (OD600 = ~ 1 to ~ 3); ETH, ethanol growth phase (OD600 > 10). As the peak is not found, the protein is not identified in LC-MS/MS proteomics samples. Means ± standard deviation are shown ($N = 3$); *, $N = 2$ (found in two out of three samples) and means ± absolute errors are shown; and #, $N = 1$ (found in one out of three samples).

The promoter activities and proteomics abundances of the eight selected targets follow the same change patterns (Fig. 5a and b). However, the normalized protein abundances from proteomics data do not quantitatively align with the fluorescence levels of the yEGFP expressed under the control of their promoters (Fig. 5 and Supplementary Fig. 3). We found that GFP fluorescence levels have a better correlation with the square roots of normalized protein abundances (Supplementary Fig. 3; $R^2 = 0.85$) than with the normalized protein abundances (Fig. 5b; $R^2 = 0.77$). Such square-root rescaling can make the protein abundance fold-changes into the magnitudes seen through the GFP reporter system. Square-root transformation has the effects of reducing the skewness of data distribution and transforming a non-linear relationship into a linear one. We are uncertain about whether the square-root transformation implies any biological principles. As aforementioned, protein expression levels are regulated at multiple levels, not only through the transcription efficiency of the promoter, but also through the efficiency of the terminator, mRNA stability, translation efficiency, and protein stability. The methods for converting mass spectrometry intensities to absolute protein abundances also have different effects on data accuracy [75]. The GFP fluorescence was standardized to the auto-fluorescence at the single-cell levels, while protein abundances of different samples were standardized to the equal total sum. These may influence the precise interpretation of proteomics data.

Mdh2 abundances and the GFP expression levels from the *MDH2* promoter were low in the cells at the exponential growth phase and increased after the diauxic shift into the ethanol growth phase (Fig. 5). The fold-changes of the normalized protein abundances is ~142 (~12 after square-root transformation), whereas the fold-change of the *MDH2* promoter strength is ~5. Glucose-inducible degradation of Mdh2 (half-life = 2.8 h on glucose) [76], may contribute to the larger fold-change at the protein abundance levels. Larger fold-changes of the protein abundance levels were also seen for Met16 and San1. The San1 protein half-life is 3.3 h, which might contribute to the relatively low abundance of ethanol. In comparison, Tdh3 half-life is 13 h, Tef1 10 h, yEGFP 7 h, and Adh1 6 h [77]. Protein stability might have an important effect on the protein abundances examined through GFP fluorescence and mass spectrometry intensity.

Hxk2 depletion caused a decrease in Hxt1 abundance during the exponential growth phase. Consistently, the GFP fluorescence from the *HXT1* promoter in the *hxk2*Δ background was ~2.9-fold lower than that in *HXK*-wildtype background. This fold-change was slightly larger than the fold-change caused by growth on ethanol (~2.2 fold; Fig. 5a).

As opposed to the protein abundance data, the *HXT* promoter activities were still dependent on glucose availability in the *hxk2*Δ background. The *HXT1* promoter activity in *hxk2*Δ strain decreased by ~4.9-fold in the ethanol growth phase, in comparison with the exponential growth phase. This is consistent with the fact that the *HXT1* promoter inducer Rgt1 is co-regulated through Hxk2/Snf1-depedent mechanism and Mth1-dependent mechanism [78–80]. This indicates that the *HXT1* promoter responds to glucose in the *hxk2*Δ background and can also be used as the regulatory promoter for dynamic metabolic control. However, this process needs to be optimized case-by-case so that the decreased expression from the *HXT*1 promoter does not impact the cell growth negatively when used to control the expression of essential metabolic genes.

4. Conclusion

In summary, we elaborated the proteomics responses to Hxk2 depletion and growth on ethanol to illustrate Hxk2-dependent and Hxk2-independent genetic regulations in *S. cerevisiae*. The proteomics data are consistent with previous classical genetics studies, showing that Hxk2 disruption can lift glucose repression on alternative carbon source catabolism and respiratory metabolism. This validates our previous hypothesis that depleting Hxk2 may upregulate *GAL* promoters-controlled heterologous synthetic pathways for improved nerolidol production. In some scenarios, disrupting *HXK2* may be adapted to increase the TCA cycle and electron transport train functions in metabolic engineering.

Amino acid anabolic pathways respond to Hxk2 depletion and growth on ethanol in a variety of patterns. Branched amino acids and arginine synthetic enzymes are downregulated in response to Hxk2 depletion, and several lysine synthetic enzymes and sulfate-assimilating enzymes are downregulated in response to growth on ethanol but not to Hxk2 depletion. This further supports the hypothesis that there are Hxk2-dependent and Hxk2-independent crosstalk mechanisms between carbon and nitrogen regulatory pathways [81,82].

Seventeen transcription factors were enriched and found to be associated with protein expression upregulation in response to Hxk2 depletion and growth on ethanol. They include documented transcription factors important for glucose repression and additional nine factors, which functions in glucose repression are not confirmed. It is challenging to bring a precise regulatory landscape of these transcription factors to confirm their roles in the upregulation responses. The enriched transcription factors share common regulatory targets and have many “potential” regulatory targets unconfirmed or undocumented. Co-regulation of multi-factors, epigenetic regulation, epistatic regulation, and post-transcriptional regulation, further add the complexity for detailing the regulatory networks. More shared -omics data, a better genome-scaled regulatory network model, and an advanced computational capacity, are all important for a comprehensive analysis of the genetic responses to genetic or environmental perturbation.

The genetic responses observed from the proteomics data are consistent with many previous studies [46,47,44]. We particularly validated the activities of the promoters of several regulatory targets. The *RIM4* promoter is co-regulated by Hxk2-dependent mechanisms and Ash1- and-Ume6-mediated repression. The *HXT1* promoter is downregulated in response to *hxk2* deletion, but still exhibits the glucose-dependent activation features in the *hxk2*Δ background. Future application of the *HXT1* promoter in an *Hxk2-depleted* or *hxk2*Δ background should be carefully titrated.

Declaration of Competing Interest

CEV declares competing interests in EDEN BREW (Australia). Others declare that they have no known competing financial interests or personal relationships that could have appeared to influence the work reported in this paper.

CRediT authorship contribution statement

Zeyu Lu: Investigation, Methodology, Validation, Conceptualization, Writing – original draft. **Qianyi Shen:** Investigation, Validation, Conceptualization, Methodology, Writing – original draft. **Lian Liu:** Data curation, Methodology, Writing – original draft. **Gert Talbo:** Data curation, Methodology. **Robert Speight:** Supervision, Resources, Investigation. **Matt Trau:** Supervision, Resources, Investigation, Project administration. **Geoff Dumsday:** Supervision, Resources, Investigation, Funding acquisition. **Christopher B. Howard:** Supervision, Resources, Investigation. **Claudia E. Vickers:** Supervision, Resources, Formal analysis, Investigation, Funding acquisition. **Bingyin Peng:** Investigation, Methodology, Conceptualization, Formal analysis, Funding acquisition, Supervision, Writing – original draft.

Acknowledgement

B.P. and a part of this work were financially supported by CSIRO and the University of Queensland in the form of a Synthetic Biology Future Science Platform Fellowship. A part of this work was financially supported by Australian Research Council centre of Excellence in Synthetic Biology (CE200100029), which is funded by the Australian Government. Metabolomics Australia is supported by BioPlatforms Australia through the Commonwealth Government’s National Collaborative Research Infrastructure Strategy (NCRIS).

Supplementary materials

Supplementary material associated with this article can be found, in the online version, at doi:10.1016/j.engmic.2023.100079.

References

[1] P. Cai, X. Wu, J. Deng, L. Gao, Y. Shen, L. Yao, Y.J. Zhou, Methanol biotransformation toward high-level production of fatty acid derivatives by engineering the industrial yeast Pichia pastoris, Proc. Natl. Acad. Sci. 119 (2022) e2201711119.
[2] G. Liu, Y. Qu, Integrated engineering of enzymes and microorganisms for improving the efficiency of industrial lignocellulose deconstruction, Eng. Microbiol. 1 (2021) 100005.
[3] T. Liu, B. Peng, S. Huang, A. Geng, Recombinant xylose-fermenting yeast construction for the co-production of ethanol and cis,cis-muconic acid from lignocellulosic biomass, Bioresource Technol. Rep. 9 (2020) 100395.
[4] Y. Liu, P. Cruz-Morales, A. Zargar, M.S. Belcher, B. Pang, E. Englund, Q. Dan, K. Yin, J.D. Keasling, Biofuels for a sustainable future, Cell 184 (2021) 1636–1647.
[5] J.H. Collins, K.W. Keating, T.R. Jones, S. Balaji, C.B. Marsan, M. Çomo, Z.J. Newlon, T. Mitchell, B. Bartley, A. Adler, N. Roehner, E.M. Young, Engineered yeast genomes accurately assembled from pure and mixed samples, Nat. Commun. 12 (2021) 1485.
[6] M. Liu, J. Zhang, J. Ye, Q. Qi, J. Hou, Morphological and metabolic engineering of yarrowia lipolytica to increase β-carotene production, ACS Synth. Biol. 10 (2021) 3551–3560.
[7] B. Peng, L. Esquirol, Z. Lu, Q. Shen, L.C. Cheah, C.B. Howard, C. Scott, M. Trau, G. Dumsday, C.E. Vickers, An *in vivo* gene amplification system for high level expression in Saccharomyces cerevisiae, Nat. Commun. 13 (2022) 2895.
[8] S. Shi, N. Qi, J. Nielsen, Microbial production of chemicals driven by CRISPR-Cas systems, Curr. Opin. Biotechnol. 73 (2022) 34–42.
[9] J. Nielsen, Jay D. Keasling, Engineering cellular metabolism, Cell 164 (2016) 1185–1197.
[10] R.H. De Deken, The crabtree effect: a regulatory system in, Yeast. Microbiol. 44 (1966) 149–156.
[11] L. Geistlinger, G. Csaba, S. Dirmeier, R. Küffner, R. Zimmer, A comprehensive gene regulatory network for the diauxic shift in Saccharomyces cerevisiae, Nucle. Acids Res. 41 (2013) 8452–8463.
[12] F. Rolland, J. Winderickx, J.M. Thevelein, Glucose-sensing mechanisms in eukaryotic cells, Trends Biochem. Sci. 26 (2001) 310–317.
[13] X. Jiao, Y. Gu, P. Zhou, H. Yu, L. Ye, Recent advances in construction and regulation of yeast cell factories, World J. Microbiol. Biotechnol. 38 (2022) 57.
[14] B. Peng, R.J. Wood, L.K. Nielsen, C.E. Vickers, An Expanded Heterologous GAL Promoter Collection For Diauxie-Inducible Expression in Saccharomyces cerevisiae, ACS Synthetic Biology, 2018.
[15] Y. Zhao, Y. Zhang, J. Nielsen, Z. Liu, Production of β-carotene in Saccharomyces cerevisiae through altering yeast lipid metabolism, Biotechnol. Bioeng. 118 (2021) 2043–2052.
[16] B. Peng, M.R. Plan, A. Carpenter, L.K. Nielsen, C.E. Vickers, Coupling gene regulatory patterns to bioprocess conditions to optimize synthetic metabolic modules for improved sesquiterpene production in yeast, Biotechnol. Biofuels 10 (2017) 43.

[17] B. Peng, T. Williams, M. Henry, L. Nielsen, C. Vickers, Controlling heterologous gene expression in yeast cell factories on different carbon substrates and across the diauxic shift: a comparison of yeast promoter activities, Microb. Cell Fact. 14 (2015) 91.
[18] D. Ahuatzi, A. Riera, R. Pelaez, P. Herrero, F. Moreno, Hxk2 regulates the phosphorylation state of Mig1 and therefore its nucleocytoplasmic distribution, J. Biol. Chem. 282 (2007) 4485–4493.
[19] J.A. Diderich, L.M. Raamsdonk, A.L. Kruckeberg, J.A. Berden, K. Van Dam, Physiological properties of Saccharomyces cerevisiae from which hexokinase II has been deleted, Appl. Environ. Microbiol. 67 (2001) 1587–1593.
[20] A. Kummel, J.C. Ewald, S.M. Fendt, S.J. Jol, P. Picotti, R. Aebersold, U. Sauer, N. Zamboni, M. Heinemann, Differential glucose repression in common yeast strains in response to HXK2 deletion, FEMS Yeast Res. 10 (2010) 322–332.
[21] Z. Lu, B. Peng, B.E. Ebert, G. Dumsday, C.E. Vickers, Auxin-mediated protein depletion for metabolic engineering in terpene-producing yeast, Nat. Commun. 12 (2021) 1051.
[22] J.M. Schuurmans, A. Boorsma, R. Lascaris, K.J. Hellingwerf, M.J. Teixeira de Mattos, Physiological and transcriptional characterization of Saccharomyces cerevisiae strains with modified expression of catabolic regulators, FEMS Yeast Res. 8 (2008) 26–34.
[23] J.M. Schuurmans, S.L. Rossell, A. van Tuijl, B.M. Bakker, K.J. Hellingwerf, M.J. Teixeira de Mattos, Effect of hxk2 deletion and HAP4 overexpression on fermentative capacity in Saccharomyces cerevisiae, FEMS Yeast Res. 8 (2008) 195–203.
[24] H. Chen, X. Chai, Y. Wang, J. Liu, G. Zhou, P. Wei, Y. Song, L. Ma, The multiple effects of REG1 deletion and SNF1 overexpression improved the production of S-adenosyl-L-methionine in Saccharomyces cerevisiae, Microb. Cell Fact. 21 (2022) 174.
[25] A. Kümmel, J.C. Ewald, S.-.M. Fendt, S.J. Jol, P. Picotti, R. Aebersold, U. Sauer, N. Zamboni, M. Heinemann, Differential glucose repression in common yeast strains in response to HXK2 deletion, FEMS Yeast Res. 10 (2010) 322–332.
[26] M.A. Lalwani, E.M. Zhao, J.L. Avalos, Current and future modalities of dynamic control in metabolic engineering, Curr. Opin. Biotechnol. 52 (2018) 56–65.
[27] O.M. Koivistoinen, J. Kuivanen, D. Barth, H. Turkia, J.P. Pitkänen, M. Penttilä, P. Richard, Glycolic acid production in the engineered yeasts Saccharomyces cerevisiae and Kluyveromyces lactis, Microb. Cell Fact. 12 (2013) 82.
[28] I.F. Hayat, M. Plan, B.E. Ebert, G. Dumsday, C.E. Vickers, B. Peng, Auxin-mediated induction of GAL promoters by conditional degradation of Mig1p improves sesquiterpene production in Saccharomyces cerevisiae with engineered acetyl-CoA synthesis, Microb. Biotechnol. 14 (2021) 2627–2642.
[29] B. Peng, N.C. Bandari, Z. Lu, C.B. Howard, C. Scott, M. Trau, G. Dumsday, C.E. Vickers, Engineering eukaryote-like regulatory circuits to expand artificial control mechanisms for metabolic engineering in Saccharomyces cerevisiae, Commun. Biol. 5 (2022) 135.
[30] Y. Zhang, M. Su, Z. Wang, J. Nielsen, Z. Liu, Rewiring regulation on respiro-fermentative metabolism relieved Crabtree effects in Saccharomyces cerevisiae, Synth. Syst. Biotechnol. 7 (2022) 1034–1043.
[31] H. Moriya, M. Johnston, Glucose sensing and signaling in Saccharomyces cerevisiae through the Rgt2 glucose sensor and casein kinase I, Proc. Natl. Acad. Sci. 101 (2004) 1572–1577.
[32] S. Cheng, X. Liu, G. Jiang, J. Wu, J.-l. Zhang, D. Lei, Y.J. Yuan, J. Qiao, G.R. Zhao, Orthogonal engineering of biosynthetic pathway for efficient production of limonene in saccharomyces cerevisiae, ACS Synth. Biol. 8 (2019) 968–975.
[33] G. Scalcinati, S. Partow, V. Siewers, M. Schalk, L. Daviet, J. Nielsen, Combined metabolic engineering of precursor and co-factor supply to increase α-santalene production by Saccharomyces cerevisiae, Microb. Cell Fact. 11 (2012) 117.
[34] J. Zhao, C. Li, Y. Zhang, Y. Shen, J. Hou, X. Bao, Dynamic control of *ERG20* expression combined with minimized endogenous downstream metabolism contributes to the improvement of geraniol production in *Saccharomyces cerevisiae*, Microb. Cell Fact. 16 (2017) 17.
[35] A. Kaniak, Z. Xue, D. Macool, J.H. Kim, M. Johnston, Regulatory network connecting two glucose signal transduction pathways in saccharomyces cerevisiae, Eukaryotic Cell 3 (2004) 221–231.
[36] F. Rolland, E. Baena-Gonzalez, J. Sheen, Sugar sensing and signaling in plants: conserved and novel mechanisms, Annu. Rev. Plant Biol. 57 (2006) 675–709.
[37] A. Carrillo-Garmendia, C. Martinez-Ortiz, J.G. Martinez-Garfias, S.E. Suarez-Sandoval, J.C. González-Hernández, G.M. Nava, M.D. Dufoo-Hurtado, L.A. Madrigal-Perez, Snf1p/Hxk2p/Mig1p pathway regulates hexose transporters transcript levels, affecting the exponential growth and mitochondrial respiration of Saccharomyces cerevisiae, Fungal Genet. Biol. 161 (2022) 103701.
[38] M. Ashburner, C.A. Ball, J.A. Blake, D. Botstein, H. Butler, J.M. Cherry, A.P. Davis, K. Dolinski, S.S. Dwight, J.T. Eppig, M.A. Harris, D.P. Hill, L. Issel-Tarver, A. Kasarskis, S. Lewis, J.C. Matese, J.E. Richardson, M. Ringwald, G.M. Rubin, G. Sherlock, Gene ontology: tool for the unification of biology. The gene ontology consortium, Nat. Genet. 25 (2000) 25–29.
[39] T.G.O. Consortium, The gene ontology resource: enriching a gold mine, Nucle. Acids Res. 49 (2020) D325–D334.
[40] P.T. Monteiro, J. Oliveira, P. Pais, M. Antunes, M. Palma, M. Cavalheiro, M. Galocha, C.P. Godinho, L.C. Martins, N. Bourbon, M.N. Mota, R.A. Ribeiro, R. Viana, I. Sá-Correia, M.C. Teixeira, YEASTRACT+: a portal for cross-species comparative genomics of transcription regulation in yeasts, Nucle. Acids Res. 48 (2020) D642–D649.
[41] T.N. Mavrich, I.P. Ioshikhes, B.J. Venters, C. Jiang, L.P. Tomsho, J. Qi, S.C. Schuster, I. Albert, B.F. Pugh, A barrier nucleosome model for statistical positioning of nucleosomes throughout the yeast genome, Genome Res. 18 (2008) 1073–1083.
[42] K.D. Entian, P. Kötter, 23 yeast mutant and plasmid collections, Methods Microbiol. 26 (1998) 431–449.
[43] B. Derrick, P. White, Why Welch's test is type I error robust, TQMP 12 (2016) 30–38.
[44] A. Rodriguez, T. De La Cera, P. Herrero, F. Moreno, The hexokinase 2 protein regulates the expression of the GLK1, HXK1 and HXK2 genes of Saccharomyces cerevisiae, Biochem. J. 355 (2001) 625–631.
[45] F.J. Boonekamp, E. Knibbe, M.A. Vieira-Lara, M. Wijsman, M.A.H. Luttik, K. van Eunen, M.D. Ridder, R. Bron, A.M. Almonacid SuaCz, P. van Rijn, J.C. Wolters, M. Pabst, J.M. Daran, B.M. Bakker, P. Daran-Lapujade, Full humanization of the glycolytic pathway in Saccharomyces cerevisiae, Cell Rep. 39 (2022) 111010.
[46] P. Herrero, C. Martínez-Campa, F. Moreno, The hexokinase 2 protein participates in regulatory DNA-protein complexes necessary for glucose repression of the SUC2 gene in Saccharomyces cerevisiae, FEBS Lett. 434 (1998) 71–76.
[47] S. Ozcan, M. Johnston, Three different regulatory mechanisms enable yeast hexose transporter (HXT) genes to be induced by different levels of glucose, Mol. Cell. Biol. 15 (1995) 1564–1572.
[48] J. Zhang, L.G. Hansen, O. Gudich, K. Viehrig, L.M.M. Lassen, L. Schrübbers, K.B. Adhikari, P. Rubaszka, E. Carrasquer-Alvarez, L. Chen, V. D'Ambrosio, B. Lehka, A.K. Haidar, S. Nallapareddy, K. Giannakou, M. Laloux, D. Arsovska, M.A.K. Jørgensen, L.J.G. Chan, M. Kristensen, H.B. Christensen, S. Sudarsan, E.A. Stander, E. Baidoo, C.J. Petzold, T. Wulff, S.E. O'Connor, V. Courdavault, M.K. Jensen, J.D. Keasling, A microbial supply chain for production of the anti–cancer drug vinblastine, Nature 609 (2022) 341–347.
[49] S.K. Hammer, J.L. Avalos, Harnessing yeast organelles for metabolic engineering, Nat. Chem. Biol. 13 (2017) 823–832.
[50] O. Foresti, A. Ruggiano, H.K. Hannibal-Bach, C.S. Ejsing, P. Carvalho, Sterol homeostasis requires regulated degradation of squalene monooxygenase by the ubiquitin ligase Doa10/Teb4, Elife 2 (2013) e00953.
[51] D. Zattas, J.M. Berk, S.G. Kreft, M. Hochstrasser, A conserved c-terminal element in the yeast Doa10 and human MARCH6 ubiquitin ligases required for selective substrate degradation, J. Biol. Chem. 291 (2016) 12105–12118.
[52] C. Zhu, K.J. Byers, R.P. McCord, Z. Shi, M.F. Berger, D.E. Newburger, K. Saulrieta, Z. Smith, M.V. Shah, M. Radhakrishnan, A.A. Philippakis, Y. Hu, F. De Masi, M. Pacek, A. Rolfs, T. Murthy, J. Labaer, M.L. Bulyk, High-resolution DNA-binding specificity analysis of yeast transcription factors, Genome Res. 19 (2009) 556–566.
[53] M.J. Carrozza, L. Florens, S.K. Swanson, W.J. Shia, S. Anderson, J. Yates, M.P. Washburn, J.L. Workman, Stable incorporation of sequence specific repressors Ash1 and Ume6 into the Rpd3L complex, Biochim. Biophys. Acta (BBA) - Gene Struct. Express. 1731 (2005) 77–87.
[54] M.E. Maxon, I. Herskowitz, Ash1p is a site-specific DNA-binding protein that actively represses transcription, Proc. Natl. Acad. Sci. U.S.A. 98 (2001) 1495–1500.
[55] C.P.C. Lin, C. Kim, S.O. Smith, A.M. Neiman, A highly redundant gene network controls assembly of the outer spore wall in S. cerevisiae, PLoS Genet. 9 (2013) e1003700.
[56] L.F. Pemberton, G. Blobel, Characterization of the Wtm proteins, a novel family of Saccharomyces cerevisiae transcriptional modulators with roles in meiotic regulation and silencing, Mol. Cell. Biol. 17 (1997) 4830–4841.
[57] R.G. Dastidar, J. Hooda, A. Shah, T.M. Cao, R.M. Henke, L. Zhang, The nuclear localization of SWI/SNF proteins is subjected to oxygen regulation, Cell Biosci. 2 (2012) 30.
[58] E. de Nadal, F. Posas, The HOG pathway and the regulation of osmoadaptive responses in yeast, FEMS Yeast Res. 22 (2022) foac013.
[59] M.C. Vallejo, P. Mayinger, Delayed turnover of unphosphorylated Ssk1 during carbon stress activates the yeast hog1 map kinase pathway, PLoS ONE 10 (2015) e0137199.
[60] C. Bai, M. Tesker, D. Melamed-Kadosh, D. Engelberg, A. Admon, Hog1-induced transcription of RTC3 and HSP12 is robust and occurs in cells lacking Msn2, Msn4, Hot1 and Sko1, PLoS ONE 15 (2020) e0237540.
[61] A.P. Capaldi, T. Kaplan, Y. Liu, N. Habib, A. Regev, N. Friedman, E.K. O'Shea, Structure and function of a transcriptional network activated by the MAPK Hog1, Nat. Genet. 40 (2008) 1300–1306.
[62] M. Gomar-Alba, M.Á. Morcillo-Parra, M.l.d. Olmo, Response of yeast cells to high glucose involves molecular and physiological differences when compared to other osmostress conditions, FEMS Yeast Res. 15 (2015) fov039.
[63] J. Gutin, A. Sadeh, A. Rahat, A. Aharoni, N. Friedman, Condition-specific genetic interaction maps reveal crosstalk between the cAMP/PKA and the HOG MAPK pathways in the activation of the general stress response, Mol. Syst. Biol. 11 (2015) 829.
[64] Klipp, E., Schaber, J., 2006. Modelling of signal transduction in yeast - sensitivity and model analysis.M. Cánovas, J.L. Iborra, A. Manjón (Eds.), Understanding and exploiting systemy biology in bioprocesses and biomedicine. Fundación Cajamurcia (2006), pp. 15-30
[65] M. de Boer, P.S. Nielsen, J.P. Bebelman, H. Heerikhuizen, H.A. Andersen, R.J. Planta, Stp1p, Stp2p and Abf1p are involved in regulation of expression of the amino acid transporter gene BAP3 of Saccharomyces cerevisiae, Nucle. Acids Res. 28 (2000) 974–981.
[66] D. Huang, H. Friesen, B. Andrews, Pho85, a multifunctional cyclin-dependent protein kinase in budding yeast, Mol. Microbiol. 66 (2007) 303–314.
[67] N. Paquin, M. Ménade, G. Poirier, D. Donato, E. Drouet, P. Chartrand, Local activation of yeast ASH1 mRNA translation through phosphorylation of Khd1p by the casein kinase Yck1p, Mol. Cell 26 (2007) 795–809.
[68] S. Raithatha, T.C. Su, P. Lourenco, S. Goto, I. Sadowski, Cdk8 regulates stability of the transcription factor phd1 to control pseudohyphal differentiation of saccharomyces cerevisiae, Mol. Cell. Biol. 32 (2012) 664–674.
[69] R. Usaite, M.C. Jewett, A.P. Oliveira, J.R. Yates Iii, L. Olsson, J. Nielsen, Reconstruction of the yeast Snf1 kinase regulatory network reveals its role as a global energy regulator, Mol. Syst. Biol. 5 (2009) 319.
[70] M.J. Carrozza, L. Florens, S.K. Swanson, W.J. Shia, S. Anderson, J. Yates, M.P. Washburn, J.L. Workman, Stable incorporation of sequence specific repressors Ash1 and

Ume6 into the Rpd3L complex, Biochim. Biophys. Acta 1731 (77–87) (2005) 75–76 discussion.
[71] E.J. Parnell, D.J. Stillman, Multiple negative regulators restrict recruitment of the SWI/SNF chromatin remodeler to the HO promoter in saccharomyces cerevisiae, Genetics 212 (2019) 1181–1204.
[72] H. Alper, C. Fischer, E. Nevoigt, G. Stephanopoulos, Tuning genetic control through promoter engineering, Proc. Natl. Acad. Sci. U. S. A. 102 (2005) 12678–12683.
[73] X. Bi, M. Braunstein, G.-J. Shei, J.R. Broach, The yeast HML I silencer defines a heterochromatin domain boundary by directional establishment of silencing, Proc. Natl. Acad. Sci. 96 (1999) 11934–11939.
[74] J.M. Weber, A.E. Ehrenhofer-Murray, Design of a minimal silencer for the silent mating-type locus HML of Saccharomyces cerevisiae, Nucle. Acids Res. 38 (2010) 7991–8000.
[75] B.J. Sánchez, P.J. Lahtvee, K. Campbell, S. Kasvandik, R. Yu, I. Domenzain, A. Zelezniak, J. Nielsen, Benchmarking accuracy and precision of intensity-based absolute quantification of protein abundances in Saccharomyces cerevisiae, Proteomics 21 (2021) 2000093.
[76] K.I. Minard, L. McAlister-Henn, Glucose-induced degradation of the MDH2 isozyme of malate dehydrogenase in yeast, J. Biol. Chem. 267 (1992) 17458–17464.
[77] R. Christiano, N. Nagaraj, F. Frohlich, T.C. Walther, Global proteome turnover analyses of the Yeasts S. cerevisiae and S. pombe, Cell Rep. 9 (2014) 1959–1965.
[78] D.P. Brink, C. Borgström, V.C. Persson, K. Ofuji Osiro, M.F. Gorwa-Grauslund, D-xylose sensing in saccharomyces cerevisiae: insights from D-glucose signaling and native D-xylose utilizers, Int. J. Mol. Sci. 22 (2021) 12410.
[79] S. Kuttykrishnan, J. Sabina, L.L. Langton, M. Johnston, M.R. Brent, A quantitative model of glucose signaling in yeast reveals an incoherent feed forward loop leading to a specific, transient pulse of transcription, Proc. Natl. Acad. Sci. 107 (2010) 16743–16748.
[80] A. Palomino, P. Herrero, F. Moreno, Tpk3 and Snf1 protein kinases regulate Rgt1 association with Saccharomyces cerevisiae HXK2 promoter, Nucle. Acids Res. 34 (2006) 1427–1438.
[81] A. González, M.N. Hall, Nutrient sensing and TOR signaling in yeast and mammals, EMBO J. 36 (2017) 397–408.
[82] S. Shashkova, N. Welkenhuysen, S. Hohmann, Molecular communication: crosstalk between the Snf1 and other signaling pathways, FEMS Yeast Res. 15 (2015) fov026.